Chinese Chemical Letters 35 (2024) 108571

Contents lists available at ScienceDirect

Chinese Chemical Letters

journal homepage: www.elsevier.com/locate/cclet

Towards catalytic reactions of Cu single-atom catalysts: Recent progress and future perspective

Yitao Zhao [a,b,*], Lei Tao [a,b]

[a] Jiangsu Province Engineering Research Center of Special Functional Textile Materials, Changzhou Vocational Institute of Textile and Garment, Changzhou 213164, China

[b] Jiangsu Key Laboratory of Advanced Catalytic Materials and Technology, Advanced Catalysis and Green Manufacturing Collaborative Innovation Center, School of Petrochemical Engineering, Changzhou University, Changzhou 213164, China

ARTICLE INFO

Article history:
Received 30 January 2023
Revised 5 May 2023
Accepted 11 May 2023
Available online 13 May 2023

Keywords:
Cu SACs
Energy conversion
Catalysis
Coordination environment

ABSTRACT

One of the urgent and challenging topics in diversified sustainable energy conversion is the development of high-performance, low-cost, and well durable catalysts. Cu single-atom catalysts (SACs) have become promising catalysts for diversified sustainable energy conversion due to their capability to maximize the utilization efficiency, acquire modulated electronic structure and optimized binding strength with intermediates. In this review, we have provided an interview of the recent progress achieved in the field of electrocatalysis, photocatalysis, and heterogeneous reaction based on Cu SACs. Started by this review, we have summarized some advanced synthetic strategies for the construction of Cu SACs. Subsequently, the performance-improving strategies are discussed in terms of the coordination environments of the reaction center, reaction mechanism and selectivity, based on free energy diagram and electron structure analysis. Finally, the remaining issues, challenges, and opportunities of Cu SACs are also provided, affording a perspective for future studies. This review not only offers us a deep understanding on the catalytic mechanism of Cu SACs for energy conversion, but also encourages more endeavors in prompting their practical application.

1. Introduction

The increasingly exhausted conventional fossil fuels and pollution problems generated an ongoing challenge facing us now [1,2]. One of the most promising strategies to address this is to explore advanced energy conversion technologies (*e.g.*, fuel cells, electrolytic cells, and metal-air batteries), which can convert chemical energy into electricity energy [3–7]. However, the conversion efficiency is closely related to the catalytic performance of catalysts. To date, the most effective candidates for catalysts are noble-metal-based materials (*e.g.*, Pt, Pd, Ru, Rh, and Ir) [8–10]. Unfortunately, their high price and low nature reserves seriously impeded their widespread application. In this regard, exploring low-cost and nature abundant candidates to substitute these noble metals is highly imperative. Recently, transition metal-based catalysts emerge as a rising star wherein a well-adjusted D-band center will give rise to promising catalytic performance [10–13]. Among various transition metals, Cu and Cu-based nanomaterials are appearing as ideal alternatives to drive not only electrocatalytic energy conversion but also heterogeneous catalysis due to its high intrinsic activity, low cost, and extraordinary durability [14–18].

As is well known to all, the catalytic performance of a catalyst is associated with the number of active sites and the intrinsic activity of individual active site [19,20]. Thus, enlarging the active area and maximizing the atomic utilization may be a favorable method to improve the catalytic performance of a catalyst [21,22]. Recently, single-atom catalysts (SACs), emerge as a rising star in the field of catalysis, has attracted increasing interest [23–25]. For one thing, SACs not only increase the number of active sites accessible for reactants and intermediates, but also largely improve the intrinsic activity of individual active site [26–28]. For another, the strong metal-support interaction can also significantly improve the catalytic activity and stability, enabling the SACs to be desirable catalysts for energy conversion and environment catalysis [29]. In this contribution, Cu SACs are thus appealing increasing interest for functioning as promising catalysts for energy conversion. Compared with traditional Cu catalysts, the highly uniform active sites and geometric configuration of Cu SACs endow them with similar electronic and spatial interaction with substrate molecule. In

* Corresponding author at: Jiangsu Province Engineering Research Center of Special Functional Textile Materials, Changzhou Vocational Institute of Textile and Garment, Changzhou 213164, China.
E-mail address: zhuomuniao2370@gmail.com (Y. Zhao).

https://doi.org/10.1016/j.cclet.2023.108571
1001-8417/

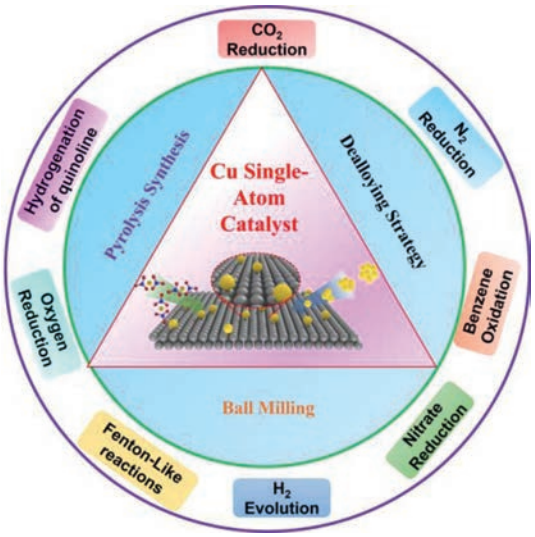

Scheme 1. Schematic illustration of the main content of this review.

addition, Cu SACs not only inherit the merits of easy separation and excellent recyclability of heterogeneous catalysts but also have the advantages of highly uniform active centers and tunable coordination environment of homogeneous catalysts [30]. Moreover, structural homogeneity of SASC favors to characterize and identify the exact atomic structure of active sites and further establishes a definitive correlation with catalytic performance [31].

By taking inspiration from these advantageous merits, Cu SACs are thus emerging as promising catalysts and attracting great interest for driving some key reactions, such as electrocatalytic energy conversion (*e.g.*, electrocatalytic CO_2 reduction, oxygen reduction reaction, nitrogen reduction reaction, and nitrate reduction reaction), photocatalytic reaction (*e.g.*, photocatalytic CO_2 reduction and hydrogen evolution reaction) and heterogeneous reaction (*e.g.*, Fenton-Like reactions, hydrogenation of quinolone, and benzene oxidation) with remarkably high catalytic activity and good durability [32–36]. Although great progress has been achieved in the fabrication and application of Cu SACs over decades, a systematical review regarding the fabrication and application in electrocatalytic, photocatalytic, and heterogeneous reactions has been rarely summarized.

Inspired by this, we provide here an overview regarding the recent progress of Cu SACs in the field of catalytic reactions (Scheme 1). We first illustrate a detailed discussion about the synthesis of advanced Cu SACs, and then some representative examples for the electrocatalytic reactions, photocatalytic reactions, and heterogeneous reactions are also summarized and compared. We also provide the theoretical insights into the coordination environment and free energy diagram analysis, which is beneficial to understand the relationship between the properties and local atomic structure, revealing reaction mechanism and guiding experiments. Finally, the challenging issues and perspective insights are presented, providing an outlook for future research.

2. Synthesis of Cu single-atom catalysts

2.1. Pyrolysis synthesis

Pyrolysis synthesis is one of the most effective strategies to prepare Cu SACs with both high catalytic activity and good durability. Pyrolysis synthesis also shows great advantages, such as optimal metal loading and nanostructure engineering, which are crucial to determining the catalytic performance. Metal-organic frameworks (MOFs) are widely applied as precursors in high-temperature pyrolysis in view of its richness in structural diversity, high porosity, tailorable composition, and multifunctionality. For example, Fu and coworkers [37] synthesized the atomically dispersed Cu-N_4 and Zn-N_4 on the N-doped carbon support (Cu/Zn-NC) *via* directly pyrolyzing CuZn-ZIF precursor (Fig. 1a). The CoZn-ZIF enabled the Cu/Zn-NC with porous skeleton and good coordination environment. Besides MOFs, other carbon-based materials, such as Cu phthalocyanine (CuPc), carbon nanotube, graphene, can also be employed as precursors or supports for yielding the Cu SACs. Cui *et al.* [38] have synthesized a Cu SAC using CuPc as the precursor and carbon nanotubes as carriers through a facile pyrolysis method. The as-prepared Cu SACs can exhibit outstanding electrocatalytic performance towards oxygen reduction reaction (ORR).

2.2. Dealloying strategy

Dealloying is also an effective strategy for the synthesis of metal-supported alloy SACs. For example, Zhao *et al.* [39] proposed a facile dealloying strategy to synthesize the atomic Cu dispersed on hierarchically porous gold architectures (denoted as np-Cu_1Au SAA) (Fig. 1b). Remarkably, the resulting np-Cu_1Au SAA with rich active sites can achieve a nearly 100% CO Faraday efficiency during electrocatalytic CO_2 reduction reaction (CO_2RR). It is uncovered that the Cu-Au interface sites can function as the intrinsic active centers to facilitate the activated adsorption of CO_2 molecule and stabilize the *COOH intermediate.

2.3. Other methods

Besides pyrolysis method and dealloying strategy, some other methods such as ball milling technique, wet-chemical method, gas-transport strategy, are also proposed for the synthesis of Cu SACs. Taking Wu's work as a representative example [40], they have developed a new high-temperature gas-transport strategy to directly transform a series of commercial available metal oxides into isolated single atoms onto the nitrogen-doped carbon (NC) with ease of mass-production (Fig. 1c). To be specific, commercial Cu_2O power and NC are separately located in the porcelain boat. At a high temperature of 1273 K in flowing N_2, the surface Cu_2O is initially evaporated to form volatile species, which can be trapped and reduced by NC, yielding the isolated single-atom copper sites (Cu ISAS/NC) catalyst. Interestingly, this gas-transport strategy can also be extended to the synthesis of other M ISAS/NC (M = Mo, Sn) by varying the metal oxide precursors.

In recent years, some other effective synthesis methods are also proposed for the fabrication of highly efficient Cu SACs. Among them, the physical and chemical deposition methods have been widely developed for the successful fabrication of Cu SACs [41]. Generally, the deposition method includes the chemical vapour deposition, atomic layer deposition, and electrochemical deposition. In addition, the electron/ion irradiation method that can create surface vacancy to trap metal atoms is also another advanced strategy for the synthesis of Cu SACs [42].

3. Catalytic reactions

3.1. Electrocatalytic reactions

3.1.1. Electrocatalytic CO_2 reduction reaction

The electrocatalytic conversion of CO_2 using renewable energy sources is widely considered as a promising approach to cut down the continuous accumulation of atmospheric CO_2 and yield a supply of value-added chemical fuels to regain the carbon balance [43,44]. Because of intrinsic inertness of CO_2, the electrochemical reduction of CO_2 not only depends on the electrocatalysts that can

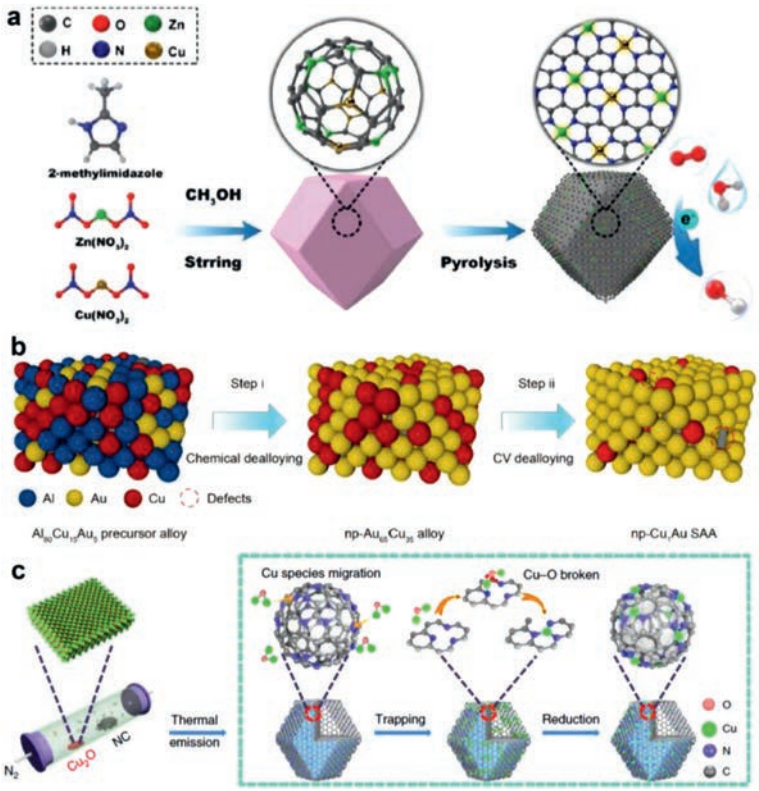

Fig. 1. (a) Schematically showing the synthetic strategies of Cu SACs by pyrolysis method. Reproduced with permission [38]. Copyright 2019, Royal Society Chemistry. (b) Scheme for the synthesis of np-Cu_1Au SAA *via* dealloying strategy. Reproduced with permission [39]. Copyright 2021, Springer. (c) Schematic illustration of the synthesis of Cu ISAS/NC *via* gas-transport strategy. Reproduced with permission [40]. Copyright 2020, Nature Publishing Group.

drive CO_2 reduction at ambient condition but also allow the formation of value-added products [45–48]. Therefore, it is necessary to develop the advanced electrocatalysts with not only high electrocatalytic activity but also desirable selectivity. Among a wide range of material candidates, Cu-based materials are well known as almost the most effective materials that can electrochemically convert CO_2 to liquid fuels with high activity and good selectivity [49,50]. However, Cu-based electrocatalysts usually generate a fairly broad mix of gaseous and liquid phase chemicals. Thus, controlling the catalytic selectivity of CO_2RR to desired product remains a forbidden challenge. Recently, Cu SACs with completely exposed active sites can exhibit ultrathin catalytic activity and selectivity of electrocatalytic CO_2RR. To this end, intensive endeavors have been devoted to the design and fabrication of high-quality Cu SACs to boost the selectively catalytic CO_2 conversion [51,52].

For example, Jiao *et al.* [53] reported the synthesis of an atom-pair catalyst (APC) that features a highly active Cu atomic interface, where the active site of APC comprises Cu_1^0-Cu_1^{x+} pairs were stabilized by the Te surface defects on $Pd_{10}Te_3$ alloy nanowires (Figs. 2a–d). It was demonstrated that the Cu_1^0-Cu_1^{x+} pairs can exhibit superb activity and high Faradaic efficiency to selectively produce CO in CO_2RR at low applied overpotentials (Figs. 2e and f). Upon combination of the density functional theorty (DFT) calculations and experimental data, it was uncovered that the outstanding electrocatalytic performance of Cu_1^0-Cu_1^{x+} pairs was ascribed to the CO_2 activation *via* a "biatomic activating bimolecular" mechanism (Figs. 2g and h), suggesting the great potential of the Cu SACs for selectively converting CO_2 to CO.

In addition to the efficient conversion of CO_2 to CO, Cu SACs are also demonstrated to be highly active towards the production of methane. Taking Zheng's work as a representative example [51], they constructed a Cu, N-codoped carbon nanosheet structure by atomically fabricating the single atom distribution of Cu-N_x coordination with varied Cu doping concentrations. The obtained single-atom Cu-N_x coordination structure is demonstrated to be highly effective for the electrocatalytic CO_2RR to hydrocarbons, including CH_4 and C_2H_4. Remarkably, at a high Cu loading density (4.9% mol), Cu atoms were close enough to each other to enhance the C–C coupling, thus leading to ethylene as a main CO_2 reduction product. When the Cu loading density was reduced to 2.4% mol, the C1 pathway was then favored and the main CO_2 reduction product was tuned to methane, implying a tailorable approach for Cu SACs for different CO_2RR selectivity. DFT calculations revealed that the two adjacent Cu-N_2 sites binding with two CO intermediates can lead to the formation of C_2H_4, while the isolated Cu-N_4, the neighboring Cu-N_4, and the isolated Cu-N_2 sites resulted in the production of CH_4. Cai *et al.* [54] synthesized the carbon-dots-based SAC margined with unique CuN_2O_2 sites to successfully modify the electronic structures of center atoms on SACs for lowering the overall endothermic energy of key intermediates (Figs. 3a–d). Interestingly, the oxygen ligands can induce remarkably high Faradaic efficiency (78%) and selectivity (99%) for converting CO_2 to CH_4 with a current density of 40 mA/cm^2. Theoretical calculations suggested that the high selectivity and activity on CuN_2O_2 active sites are originated from the proper elevated CH_4 and H_2 energy barrier (Fig. 3e). These works suggested that the crucial role in tailoring the coordination environment to improve the selectivity of Cu SACs for electrocatalytic CO_2RR.

Moreover, Cu SACs are also demonstrated to be highly active and selective towards the electrocatalytic reduction of CO_2 to liquid fuels, such as formic acid, methanol. For instance, Zheng *et al.* [55] synthesized the Pb single-atom alloyed Cu catalyst (Pb_1Cu) to realize near unity selectivity of formate with record activity *via* an epoxide gelation approach. It is reported that the Pb_1Cu cata-

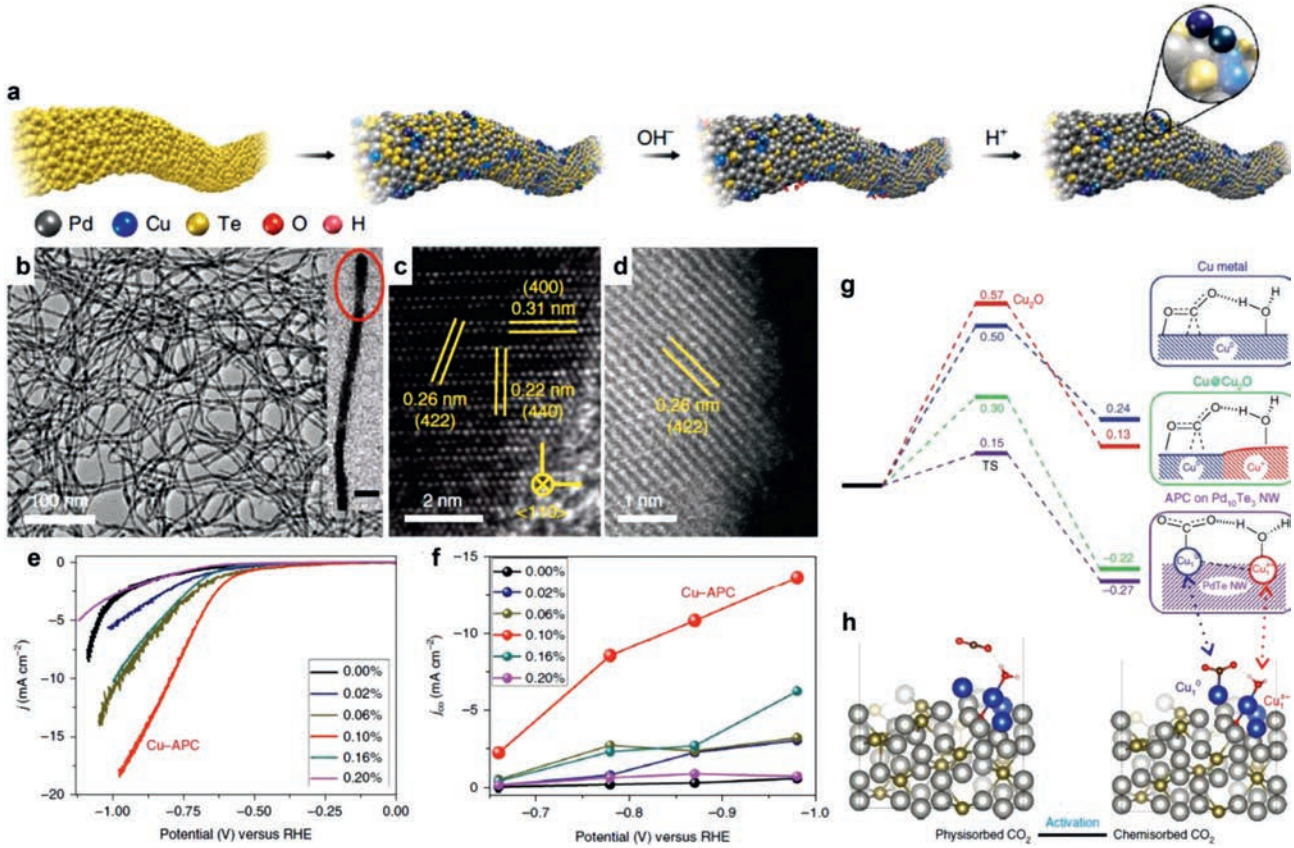

Fig. 2. (a) Scheme of the synthesis of APC. (b) TEM and (c, d) HRTEM images of the APC. (e) LSV polarization curves of APC with different amounts of Cu doping. (f) CO current densities of APC with different amounts under different potentials. (g, h) Free energy profiles for CO_2 activation mode. Reproduced with permission [53]. Copyright 2019, Nature Publishing Group.

lyst can exclusively electrochemically convert CO_2 into formate at a high current density of 1 A/cm^2 and a Faradaic efficiency ~96%. Upon combination of the *in-situ* spectroscopic evidence and theoretical calculations, it is uncovered that the activated Cu sites of the Pb_1Cu catalyst to optimize the first protonation step of the CO_2RR and divert the CO_2RR towards a HCOO* path rather than a COOH* path, thus improving the selectivity of formate. Yang *et al.* [56] synthesized the homogeneously distributed Cu single atoms on through-hole carbon nanofibers (denoted as CuSAs/TCNFs) to enable efficient electrocatalytic CO_2RR, which can generate nearly pure methanol with 44% Faradaic efficiency with −93 mA/cm^2 partial current density for C1 products and more than 50 h stability in aqueous solution. DFT calculations revealed that Cu single atoms possessed a relatively higher binding energy for *CO intermediate and further reduced them to products like methanol (Fig. 4).

3.1.2. Electrocatalytic N_2 reduction reaction

Electrocatalytic nitrogen reduction reaction (NRR) has long been regarded as a promising strategy to yield NH_3, which is critically important for both agriculture and industry [57–60]. However, its efficiency is still at a relatively low level, with poor Faradaic efficiency (FE) and being severely affected by the accompanying HER in aqueous electrolytes due to the strong N≡N triple bond (941 kJ/mol) in N_2 and high first bond cleavage energy (410 kJ/mol) [61–66]. Therefore, it is of vital importance to develop effective electrocatalysts to facilitate the cleavage of N≡N bond. Currently, noble metal Au, Ru, and Rh, are among the best performing for NRR, but their high cost and low scarcity greatly restrict their widespread and scaled up application [67]. To address this issue, nonnoble metal materials, such as MoS_2, Bi-based, and Cu-based nanocatalysts are also appearing as advanced electrocatalysts for NRR.

In recent years, SACs are emerging as promising electrocatalysts for NRR and thus extensively investigated. Indeed, single atoms that deposited on the surface of support have been demonstrated to possess several advantages, such as high atom utilization and high selectivity due to their low coordination environments. Bear these considerations into mind, intensive endeavors have been devoted to the fabrication of advanced SACs for electrocatalytic NRR, such as Fe, Co, Mo, W, Cu, and Ag SACs. Among them, Cu SACs have been reported to be highly active toward electrocatalytic NRR, along with the advantages of high intrinsic activity and low cost. For instance, Wang and coworkers reported a surfactant-free method for the successful fabrication of a new type of Cu single-atom electrocatalyst based on a porous nitrogen-doped carbon network (NC-Cu SA) (Figs. 5a–d), which was investigated for electrocatalytic NRR [58]. Impressively, NC-Cu SA can exhibit an outstanding FE of 13.8% and 11.7%, high NH_3 yield rate of ~53.3 and ~49.3 μg_{NH_3} h^{-1} mg_{cat}^{-1} in 0.1 mol/L KOH and 0.1 mol/L HCl electrolytes, respectively, surpassing the performance of Cu nanoparticle on NC. According to the mechanistic study, it is uncovered that the superb electrocatalytic performance is originated from the high density of exposed Cu-N_2 coordination and the high level of porosity (Fig. 5e).

3.1.3. Electrocatalytic oxygen reduction reaction

Electrochemical ORR has appealed increasing interest because of its irreplaceable role in energy conversion and storage, such as fuel cells and metal-air battery [68,69]. Pt and Pt-based materials are well accepted as the most effective electrocatalysts for ORR, but the high cost and low nature reserve seriously impede

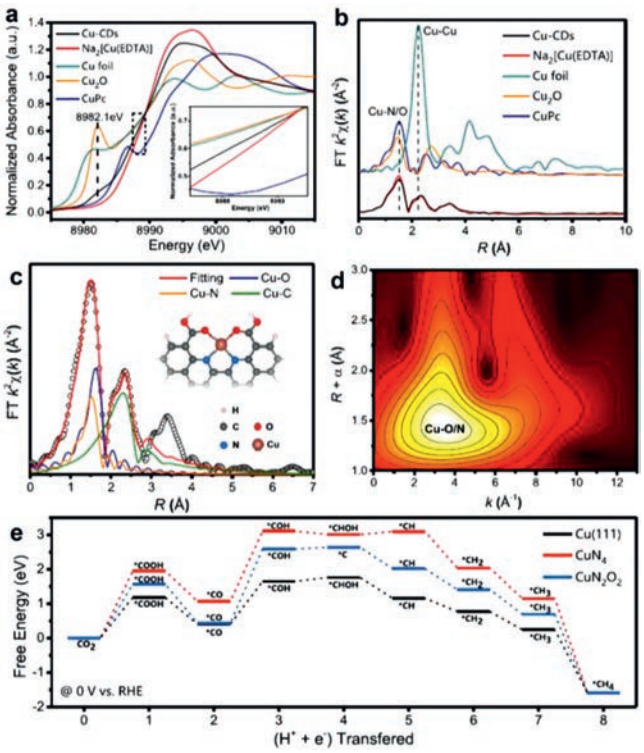

Fig. 3. (a) X-ray absorption near-edge structure (XANES) spectra and (b) Fourier transform (FT) EXAFS spectra at the Cu K-edge of different samples. (c) EXAFS fitting curves of Cu-CDs in R space using backscattering paths of Cu-N, Cu-O, and Cu-C. (d) Wavelet transform (WT) of Cu-CDs. (e) Free energy diagram of the CO_2 reduction pathway to CH_4 on the different catalysts. Reproduced with permission [54]. Copyright 2021, Nature Publishing Group.

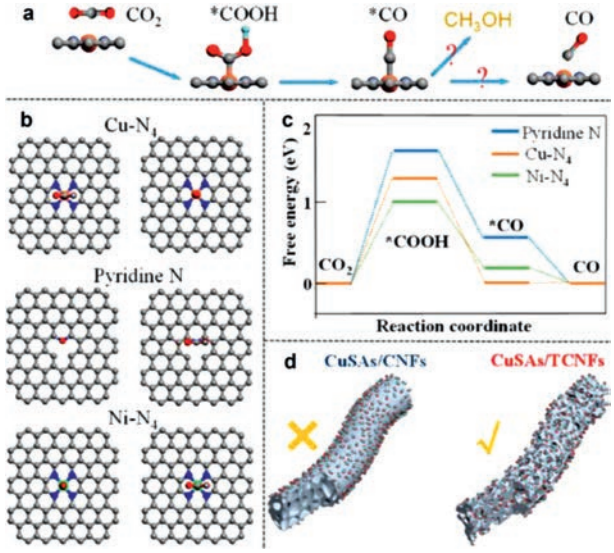

Fig. 4. (a) Optimized atomic structures of CuSAs/TCNFs and proposed reaction paths for CO_2 electroreduction. (b, c) Free energy diagram of CO_2 to CO on pyridine N, Ni-N_4, and Cu-N_4 structure. (d) Illustration of CO_2 diffusion on two samples. Reproduced with permission [56]. Copyright 2019, American Chemical Society.

their widespread application [70–77]. Therefore, developing low-cost, highly active, and durable candidate to replace traditional Pt-based materials is highly imperative [78–81]. Alternatively, non-precious metal-based metal-nitrogen-carbon (M-N-C, M stands for nonprecious metal) structures have been considered as a class of high-efficiency ORR catalysts [37,82,83]. In recent years, SAC as a rising star has made breakthroughs in energy conversion technologies with rapidly development due to the advantageous merits of highly unsaturated coordination bonds and uniform distribution of plentiful active sites [84]. Thus, the ORR activity of the M-N-C has been substantially improved by engineering the atomic site of M-N-C. Nowadays, most of the M-N-C catalysts with atomic level regulation are focusing on Fe, Co, and Ni species [85]. Atomic level Cu-N-C species are also emerging as promising catalysts for boosting the electrocatalytic reaction of CO_2RR and ORR due to high intrinsic activity and good durability [86]. Generally, the catalytic performance of Cu-N-C is determined by the number and structure of the active sites, which are critically depended on the preparation conditions. Therefore, it is urgently important to modify the coordination environment and structure of the metal active site *via* effective synthetic methods. Wang and coworkers reported that the Cu-N_2, Cu-N_3, and Cu-N_4 were all the active structure [87]. They developed a two-step method to synthesize the Cu-N-C SACs with a uniform and well-defined Cu^{2+}-N_4 structure that exhibits superb ORR activity and stability. By combining operando X-ray absorption spectroscopy with theoretical calculations, they identified the dynamic evolution of Cu-N_4 to Cu-N_3 and further to HO-Cu-N_2 under ORR working conditions, which concurrently occurred with the reduction of Cu^{2+} to Cu^{+} and was driven by the applied potential.

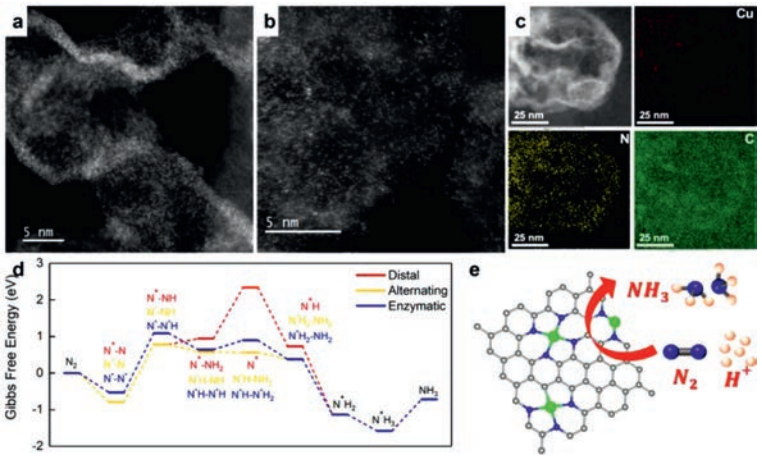

Fig. 5. (a, b) STEM and (c) elemental mapping images of the NC-Cu SA. (d) Calculated Gibbs free energies of the NRR on Cu-N_2 along the distal, alternating, and enzymatic pathways. (e) Schematically showing the NRR mechanism. Reproduced with permission [58]. Copyright 2019, American Chemical Society.

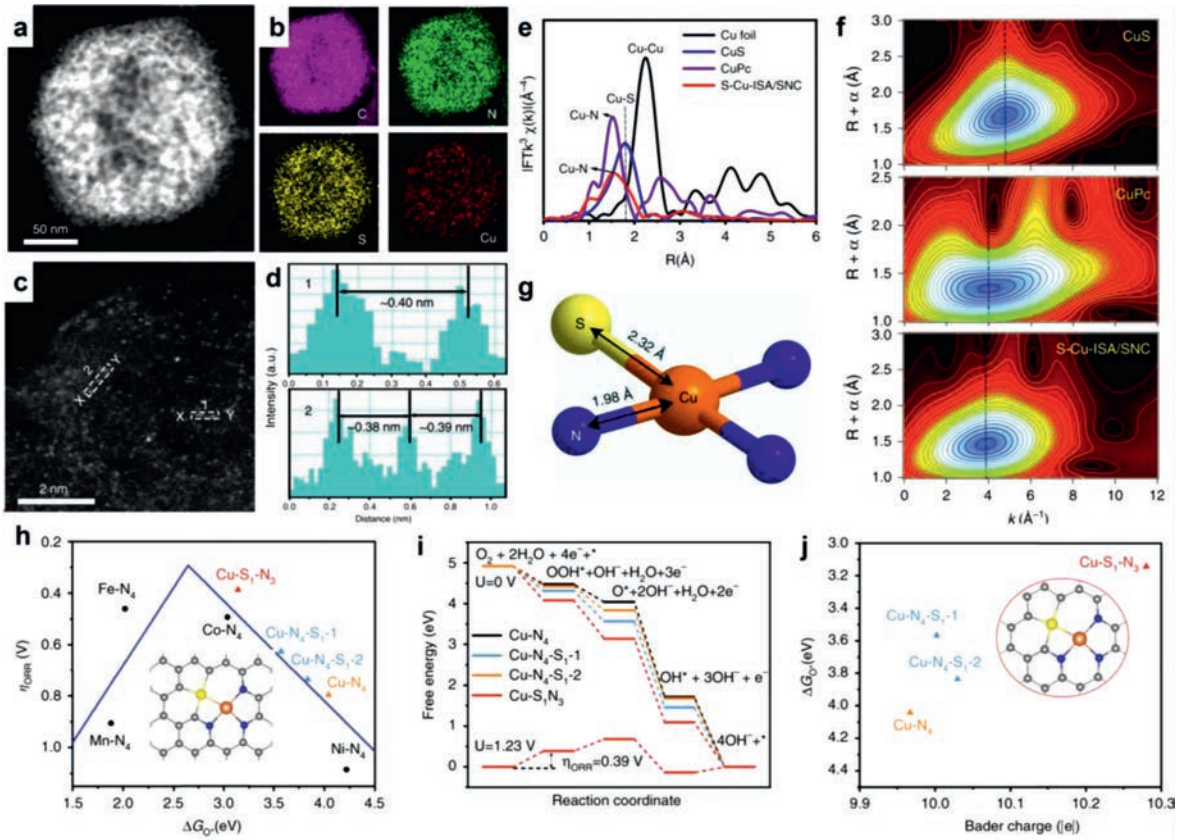

Fig. 6. (a) STEM, (b) elemental mapping, (c) high-resolution STEM, and (d) the corresponding intensity profiles along the line X-Y in (c). (e) FT k^3-weighted Cu K-edge EXAFS spectra of S-Cu-ISA/SNC and the references. (f) WT-EXAFS plots of S-Cu-ISA/SNC, CuS and CuPc. (g) Schematic atomic interface model of S-Cu-ISA/SNC. (h) ORR overpotential (η_{ORR}) as a function of O* adsorption free energy (ΔG_{O^*}) on different Cu-centered moieties. (i) Free-energy diagram for different Cu-centered moieties. (j) Relationship between the number of Bader charge of Cu and ΔG_{O^*} for different Cu-centered moieties. Reproduced with permission [88]. Copyright 2020, Nature Publishing Group.

The increase in the Cu^+/Cu^{2+} ratio with the reduced potential indicated that the low-coordinated Cu^+-N_3 was the real active site, which was further supported by theoretical calculations exhibiting the lower free energy in each elemental step of the ORR on Cu^+-N_3 than on Cu^{2+}-N_4.

Beside the Cu-N coordination, single copper atoms coordinated with both sulfur and nitrogen atoms are also demonstrated to be highly active and durable toward ORR. Taking Wang's work as a representative example [88], they synthesized a new type of Cu SACs that Cu atom was directly bonded with both sulfur and nitrogen atoms (denoted as S-Cu-ISA/SNC) by rationally controlling the unsymmetrical interface structure of central metal atoms (Figs. 6a–g). Impressively, the S-Cu-ISA/SNC is demonstrated to be highly active and durable toward ORR by delivering a half-wave potential of 0.918 V *vs.* RHE. According to the experimental data and theoretical calculation, it is revealed that the improved ORR activity is originated from the optimized atomic arrangement and density-of-states distribution of the Cu-S_1N_3 centers (Figs. 6h–j), suggesting the great influence of the coordination environment regulation on the electrocatalytic ORR performance.

The dispersing substrate is also proved to be vital in the SACs. Graphene is sp^2-hybridized carbon structure, which can serve as an ideal substrate for dispersing metal site, due to its good electrical conductivity, large specific surface area, and exceptional mechanical strength and high flexibility. Therefore, graphene-based SACs can be widely applied in driving electrocatalytic ORR. For example, Han *et al.* [89] developed a facile confined self-initiated dispersing protocol to synthesize the graphene-based Cu SACs, where the facile confined self-initiated dispersing protocol not only avoids the self-aggregation of Cu atoms, but also increase the mass loading of Cu atoms, leading to the remarkably high electrocatalytic ORR activity.

3.1.4. Electrocatalytic nitrate reduction reaction

Nitrate is one of the most widespread pollutants in surface and underground water, which is mainly emitted from artificial fertilizers in agriculture activity, factory waste disposal, and fossil fuel products of industrial effluents. Excessive nitrate emission in water has been widely recognized to pose health and environmental risks to humans, such as eutrophication and several health diseases. Electrocatalytic nitrate reduction reaction (NO_3RR) is a promising strategy for addressing these issues. Metallic Cu is also a well-known electrocatalyst for nitrate reduction reaction due to its high electrochemical activity, tunable electronic structure, and low cost [90–92]. However, some issues should be addressed before the industrial application of the electrocatalytic NO_3RR. One is the catalyst deactivation after long-time operation due to the passivation, leaching, and corrosion, the other is associated with the accumulation of nitrite, a main *quasi*-stable intermediate that is a carcinogen and more toxic than nitrate [93]. These two issues highlight the need to fabricate highly efficient, stable, and selective electrocatalyst. Downsizing the metal nanoparticles into single atoms is now appearing as a promising avenue to meet this need due to the maximized atomic utilization efficiency and high intrinsic activity [94,95]. Moreover, the strong interactions between single atoms and surrounding coordination atoms can also protect and stabilize single atomic metals, thereby significantly enhance the electrochemical stability. Therefore, Cu-based SACs are widely investigated and developed as advanced electrocatalysts for boosting electrocatalytic NO_3RR. For example, Zhu *et al.* [96] de-

signed a catalyst composed of single Cu atoms anchored on nitrogenated carbon nanosheets (Cu-N-C), which can exhibit superb activity and durability in NO_3RR with appreciably higher rates. The combined results of experimental data and DFT calculation indicate that Cu-N_2 is the key to favorable adsorption of NO_3^- and NO_2^-. This strong binding is responsible for the enhanced rate of nitrate conversion to the end products of ammonia and nitrogen. Basically, the design and synthesis of high-efficiency Cu SAC present a strategy to accelerate the reaction kinetic toward electrochemical reactions, which exhibit the potential applications of Cu SACs in energy conversion devices.

3.2. Photocatalytic reactions

3.2.1. Photocatalytic CO_2 reduction reaction

SACs, especially for Cu-based SACs, with unique electronic structure, high intrinsic activity, and distinctive coordination environments have attracted considerable attention. Besides, Cu SACs can also expose more accessible active sites and afford high atomic utilization efficiency. In this regard, Cu SACs are thus utilized as advanced photocatalysts for boosting CO_2 reduction [97,98]. Taking Wang's work as a representative example [99], they have reported a photoinduction method (PIM) to construct isolated Cu SAs (as active species) anchored on UiO-66-NH_2 to serve as photocatalyst toward CO_2 conversion to fuels. The Cu SA species can be captured by -NH_2 groups of UiO-66-NH_2 support and then anchored by after irradiation with visible light, which significantly modified the electronic structure of photocatalysts at the atomic level to facilitate the separation of electron-hole pairs. Upon the combination of experimental and theoretical data, it was revealed that the Cu SA species can induce the enrichment of the electrons on Cu SAs/UiO-66-NH_2, thus promoting the conversion of CO_2 to CHO* and CO* intermediates, leading to excellent selectivity toward methanol and ethanol.

Li *et al.* [98] synthesized the Cu SACs that anchored on the graphitic carbon nitride (g-C_3N_4) as advanced photocatalyst for catalytic CO_2RR. g-C_3N_4, as a metal-free organic photocatalyst, show outstanding properties with nearly 100% selective photocatalytic CO_2 to CO conversion, good stability, no toxicity, low cost, and a moderate band gap to harvest visible light. More importantly, it is demonstrated that the introduction of Cu atoms can work as CO_2 adsorption sites, thereby increasing the adsorption capacity of Cu-CCN samples to CO_2 (Figs. 7a–d). Moreover, theoretical calculations revealed that reducing CO_2 to CH_4 on Cu-CCN samples was an entropy-increasing process, whereas reducing CO_2 to CO was an entropy-decreasing process (Fig. 7e).

3.2.2. Photocatalytic hydrogen evolution reaction

Heterogeneous photocatalysts possess great advantages for the application in photocatalytic hydrogen evolution. To achieve high efficiency and selectivity, the electronic band structures of the co-catalysts and their interactions with light absorbers should be investigated, along with the intrinsic light-absorbing properties of the photocatalysts [100–103]. In this regard, SACs, where the isolated single atoms are anchored to the support, offer an ideal platform because of its tailorable properties by tuning the local atomic configuration [104,105]. Among various metal single atoms, Cu SACs are emerging as promising catalysts for boosting hydrogen production due to its high intrinsic activity. By taking advantages from these, intensive efforts have been devoted to the fabrication of advanced Cu SACs for boosting photocatalytic hydrogen generation. For instance, Lee *et al.* [105] reported on the design and synthesis of highly active TiO_2 photocatalysts incorporating site-specific single copper atoms (Cu/TiO_2) that exhibited a reversible and cooperative photoactivation process (Fig. 8a). Upon the combination of the experimental results and DFT calculations, it was

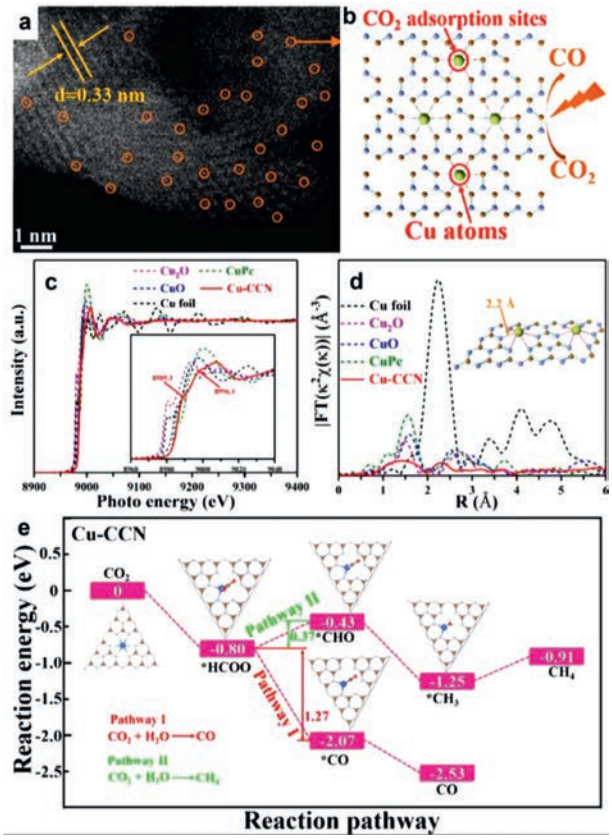

Fig. 7. (a) AC-STEM image of the Cu-CCN. (b) Schematically showing the photocatalytic CO_2 reduction based on Cu-CCN. (c) Normalized X-ray absorption near-edge structure spectra and (d) Fourier transform extended X-ray absorption fine structure spectra of the Cu-CCN, CuO, Cu_2O, CuPc, and Cu foil. (e) Reaction pathways for photocatalytic CO_2 reduction and the corresponding chemical molecular structure on Cu-CCN samples. Reproduced with permission [98]. Copyright 2019, American Chemical Society.

uncovered that the valence state of the isolated Cu atoms was changed by the atomistic localization of photogenerated electrons (Fig. 8b). This valence change can induce the activation of adjacent TiO_2, thereby tuning the initially dormant TiO_2 to an active state and greatly improving the photocatalytic performance.

Introducing Cu single atom into other light absorbers is also an effective approach to fabricate advanced Cu-based single-atom photocatalysts. Recently, polymeric carbon nitride (PCN) has also emerged as an attractive candidate for photocatalysts due to its advantageous merits, such as tunable electronic structure, good thermal and chemical stability, and environmental benignity. Therefore, incorporating Cu single atom into PCN is a promising strategy to obtain advanced photocatalysts for boosting photocatalytic hydrogen production. For instance, Zhao and coworkers [106] developed a facile molecular assembly approach to construct an intercalation-structured hollow carbon nitride sphere composed of carbon nitride nanosheets (HCNS) with atomically dispersed Cu_1N_3 moieties (Fig. 8c). According to the experimental results, it is demonstrated that the Cu_1@HCNS can exhibit superior photoredox catalysis to the pristine HCNS and the Cu_1N_3 moieties anchored on the surface of nanosheets for solar hydrogen production (3261 μmol g^{-1} h^{-1} rate) (Fig. 8d). It is uncovered that the embedded single-atom Cu can function as a modifier to greatly modify the electron structure and remarkably facilitate interfacial charge transfer of PCN. These researches have confirmed the great promise of the single-atom Cu in promoting the photocatalytic hydrogen production performance of conventional photocatalysts.

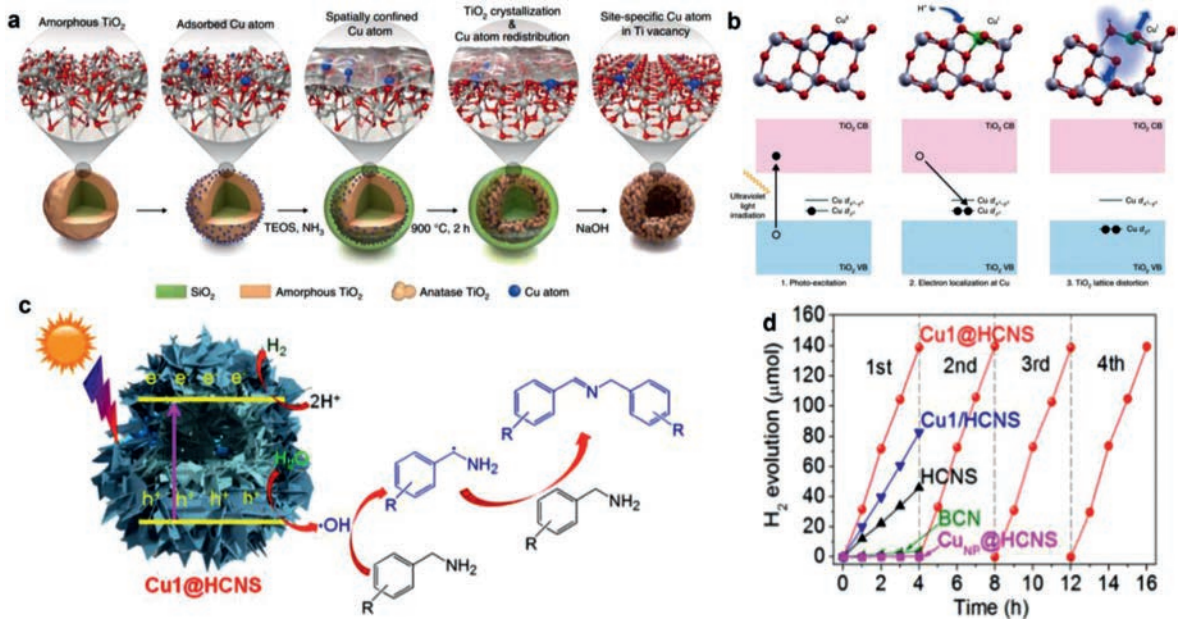

Fig. 8. (a) Schematically showing the design of a site-specific single-atom photocatalyst. (b) Schemes of the photo-excitation process. (c) Plausible reaction mechanism over Cu_1@HCNS for nonoxygen coupling of amines to imines by water under visible light irradiation. (d) Time-dependent H_2 evolution over the 3 wt% Pt-deposited samples under visible light irradiation. Reproduced with permission [105]. Copyright 2020, Nature Publishing Group.

3.3. Heterogeneous catalytic reactions

3.3.1. Fenton-Like reactions

Effective activation of hydrogen peroxide (H_2O_2) to yield reactive oxygen species (ROS) is of great importance in advanced oxidation systems. Fenton reaction is the most popular engineered avenue for ROS generation, in which H_2O_2 was decomposed into highly oxidative hydroxyl radicals (•OH) in the presence of Fe(II) [107–110]. However, conventional Fenton reaction suffers from sluggish kinetics of Fe(II) recovery and high consumption of H_2O_2 [111]. To this end, exploring advanced catalysts to improve the reaction kinetics and accelerate the reaction rate is highly imperative. In recent years, Cu-based SACs are emerging as promising catalysts for boosting the Fenton reaction due to their high intrinsic activity and maximized atomic utilization. For instance, Duan and coworkers [112] designed and synthesized a novel Cu single-atom sites coordinated onto pyrrolic N-rich g-C_3N_4 (PN-g-C_3N_4) scaffold for driving Fenton reaction. The regulated pyrrolic N-rich SA-Cu catalytic sites exhibited excellent performances for heterogeneous Fenton reaction due to the low energy barrier. Moreover, this synthetic method can also be extended to the universal synthesis of SA-TM/PN-g-C_3N_4 with remarkably high catalytic performance toward Fenton reaction.

In recent decades, sulphate radical-based oxidation reactions are also extensively explored for the degradaton of refractory organics [113]. Generally, $SO_4^{\bullet-}$ possesses a higher oxidation potential (2.5–3.1 V *vs.* NHE) and a longer half-life period (30–40 μs) than HO· (1.8–2.7 V *vs.* NHE, 20 ns); thus sulphate radicals can transfer longer distances to reach the target contaminants and mineralise them more effectively. As is well known to all, peroxymonosulphate (PMS) is a parent persulphate to produce $SO_4^{\bullet-}$ with the stimulations of ultrasound, heat, electrolysis, ultraviolet light, carbon-based materials, and transition metals [114]. PMS (also termed Oxone) is a triple salt composed of $2KHSO_5$, $KHSO_4$, and K_2SO_4. In virtue of an asymmetric structure with longer superoxide O-O bond, PMS has been believed to be an easy-handling, stable, and non toxic peroxide. Recently, a series of Cu-based SACs has been used as PMS activators for the degradation of various organic micropollutants. For example, Yang *et al.* [115] prepared the Cu-SAC with uniformed coordination structures for driving catalytic oxidation of chloroquine phosphate (CQP). It was demonstrated that the radicals ($SO_4^{\bullet-}$ and HO•) dominated the CQP oxidation (58.3%) in Cu-SAC/PMS system, which was associated with the different spin-state of the metal sites for PMS adsorption and breakage of O-O in PMS as well as the intermediates in versatile pathways, confirming the great promise of Cu SACs for sulphate radical-based oxidation reactions.

3.3.2. Hydrogenation of quinoline

Heterogeneous hydrogenation of quinoline depends on noble metal catalysts with selectivity issues or suffering from harsh reaction conditions (high temperature and high pressure of H_2). Therefore, exploring cost-effective materials to substitute noble metal catalyst is highly important. In recent years, SACs, especially for Cu-based SACs, have emerged as a class of promising candidates for boosting catalytic hydrogenation of quinoline. For example, SA Cu catalyst on N-doped carbon (CN) materials has been developed for driving the selective hydrogenation of quinoline [116]. And a compounding metal oxides (MO_x) strategy has been successfully developed to effectively change the doping type of nitrogen atoms in CN as major pyrrolic-N and pyridinic-N respectively for optimizing the catalytic performance Cu SACs in transfer hydrogenation of quinolone (Figs. 9a–c). Interestingly, the dominant pyrrolic-N in CN can improve the activity of the Cu SAC by ~2 folds to produce 1,2,3,4-tetrahydroquinoline (THQ). As a result, the Cu SAC realizes the hydrogenation of quinolines in 99% selectivity under mild conditions (60 °C for 2 h) by employing ammonia-borane (AB) as the hydrogen source, suggesting the great promise of Cu SACs for serving as catalyst toward the transfer of quinoline. Moreover, it is also reported that the superb catalytic performance is originated from the higher electron density of individual Cu centers, which facilitates the hydrogen transfer process and reduce the energy barrier (Figs. 9d–g).

3.3.3. Benzene oxidation

Owing to the unique electronic structure, remarkably enhanced intrinsic activity, and high atomic utilization, Cu-based SACs have

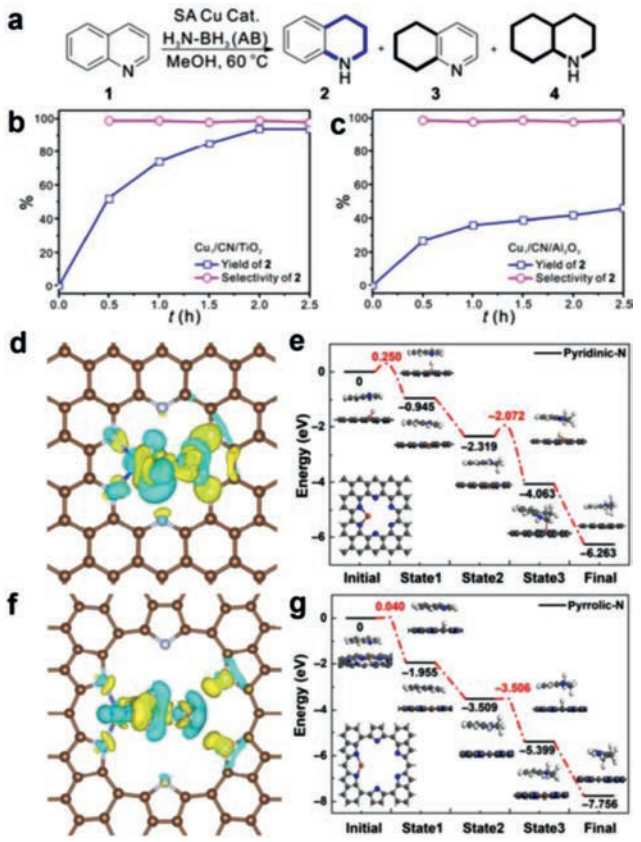

Fig. 9. (a) Mechanism for the hydrogenation of quinoline. (b, c) Kinetic studies of transfer hydrogenation of quinoline with $Cu_1/CN/TiO_2$. The differential charge density of AB molecule absorbed on SA Cu species coordinated with (d) pyridinic-N and (e) pyrrolic-N. Hydrogenation process on the coordination of (f) pyridinic-N and (g) pyrrolic-N. Reproduced with permission [116]. Copyright 2020, Springer.

thus attracted increasing interest for serving as advanced catalysts for selective oxidation of benzene to phenol [117–123]. Recent years have witnessed an explosive development of works on the fabrication of Cu-based SACs for boosting catalytic conversion of benzene to phenol [122–124]. For instance, Zhang *et al.* [124] put forward a new template-free strategy to realize the successful fabrication of porous hollow g-C_3N_4 spheres (HCNS) inlaid with single Cu atoms *via* thermal polymerization of Cu-containing supramolecular assemblies formed by the preassembly of a melamine-Cu complex with cyanuric acid. Scanning electron microscope (SEM) and transmission electron microscope (TEM) images reveal that Cu-SA/HCNS catalyst features a hollow spheral structure with *ca.* 3 nm pores (Figs. 10a and b). Extended X-Ray absorption fine structure (EXAFS) measurement indicates that Cu atoms are atomically dispersed in the HCNS matrix. The related fitting curves show a prominent peak at 1.9–2.0 Å derived from the first shell of Cu-N plus a weak contribution at 2.8–2.9 Å originating from the replacement of the second shell of Cu-N or Cu-C in the C_3N_4 model by a Cu center (Figs. 10c and d). The catalytic performance of Cu-SA/HCNS catalyst for selective oxidation of benzene to phenol is evaluated by investigating the C–H bond activation since it is of vital significance for determining the transformation efficiency. As a result, Cu-SA/HCNS catalyst shows a benzene conversion of 33.4%, with a phenol selectivity of 90.6% at 25 °C for 24 h, being much superior to the supported Cu nanoparticles. Moreover, the Cu-SA/HCNS catalyst can also exhibit superb recyclability. According to the mechanistic studies, it is revealed that the remarkably high catalytic performance is ascribed to the atomically dispersed unique Cu-N_3 species and the efficiently promoted accessibility of active sites by the porous hollow structure. Moreover, it is also disclosed that the strongly anchored Cu-N_3 species in the HCNS matrix also contributes to the excellent catalytic stability.

Recently, Wu and coworkers [35] developed a facile cation-exchange method for the successful fabrication of edge-rich S and N dual-decorated Cu SACs based on anionic frameworks of sulfides and N-rich polymer shell to generate abundant S and N defects during high-temperature annealing (Fig. 10e). Interestingly, this method can be extended to the successful fabrication of a series of highly active single-atom metal site catalyst (M SAC, M = Cu, Pt, Pd, Au, Ag, Pb, Zn, Bi, and Sb), which achieve strong metal-atom support interaction (MASI) to trap the metal by edge-rich S and N defects (Fig. 10f). Upon experiments and theoretical results, it is uncovered that the precisely obtained S, N dual-decorated Cu sites exhibit a high activity in catalytic hydroxylation of benzene at room temperature (Fig. 10g). Based on the theoretical calculations and catalytic mechanism, it is concluded that the zigzag-edged CuN_3-S-C center possesses a lower maximum reaction energy barrier (Fig. 10h), which is favorable for the thermodynamically process of the hydroxylation of benzene. Based on above results, it is easily concluded that Cu SACs hold great promise for catalyzing heteogeneous reactions, due to their inherently structural advantages and high intrinsic activity.

4. Conclusion and perspectives

This review highlights the significant progress of Cu SACs for the application in the field of electrocatalysis, photocatalysis, and heterogeneous catalysis. By manifesting some advanced synthetic strategies, such as pyrolysis, dealloying, we have summarized the preparation methods for the construction of Cu SACs with good coordination environment and modified electronic structure. Moreover, some representative Cu SACs for driving electrocatalytic, photocatalytic, and heterogeneous reaction are also discussed, aiming to provide a deep understanding on the effect of the coordination environment of copper atoms on the catalytic activity. Although the great progress of Cu SACs achieved in catalysis, some challenging issues are also existed and required to be addressed before the practical applications of Cu SACs.

First, the pyrolysis method has been demonstrated to be effective for the successful fabrication of Cu-N_x motifs, whereas the samples from the pyrolysis method are mixed with different coordination numbers. Therefore, with the aim to achieve controlled coordination atom and coordination environment, it is highly important to develop new synthetic methods.

Second, the blooming of SACs heavily depends on the development of characterization techniques. In addition, in view of the complexity in the reaction center, theoretical calculations should also be operated. Moreover, in order to monitor the reaction procedures and reaction intermediates, some *in-situ* techniques should also be conducted to gain a better understanding on the reaction mechanism.

Third, to meet the high requirement for practical application, the catalytic activity and durability of Cu SACs should also be significantly elevated. Generally, the catalytic activity and stability of SACs are associated with the mass loading of metal atoms. In this case, developing new methods to improve the mass loading of Cu atoms on the support is urgently sought. Besides, the stability of SACs has always been an enormous challenge. The poor stability of metal sites stimulate more endeavors devoted to the substantial enhancement in electrochemical stability. One of the most effective ways to enhance the stability is to yield coordination bond between support and metal atoms.

Fourth, constructing bimetallic active sites is also highly desirable to be efficient for enhancing the catalytic performance. It is believed that the coupling between the transition metal couple can

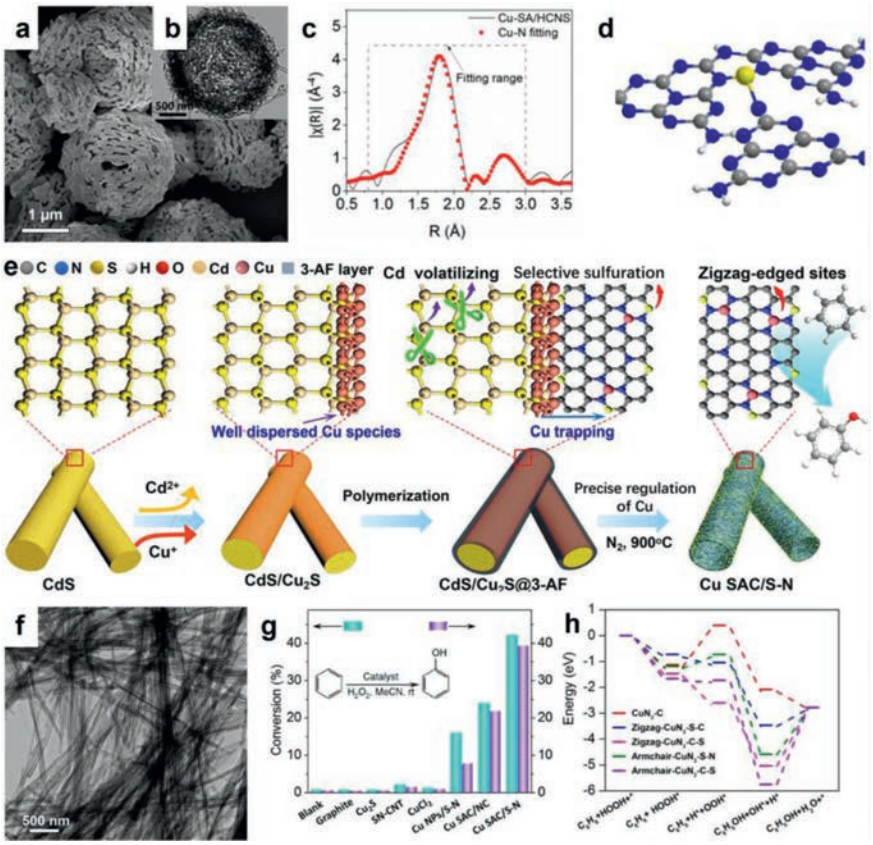

Fig. 10. (a) SEM and (b) TEM images of the Cu-SA/HCNS. (c) The corresponding EXAFS fitting curve of Cu-SA/HCNS. (d) Model of Cu–N_3 sites in Cu-SA/HCNS. Reproduced with permission [126]. Copyright 2018, American Chemical Society. (e) Scheme showing the synthetic procedures of the Cu SAC/S-N. (f) TEM image of the Cu SAC/S-N. (g) Conversion rates and yields of benzene oxidation. (h) Free energy diagram of different configurations reaction pathway. Reproduced with permission [35]. Copyright 2020, American Chemical Society.

significantly modify the electronic structure and the spin coupling of transition metal. Specifically, inducing a second transition metal can achieve a more appropriate D-band center, giving rise to satisfied catalytic performance. Moreover, the extra metal is prone to improving the catalytic stability because it might sacrifice as the reaction center of side reactions. Taking consideration of the diversity of coordination environments, great opportunity is foreseeable in Cu-based bimetal reaction center.

It is foreseen that the continued endeavors in the Cu SACs will greatly narrow the gap between laboratory catalyst and commercial counterparts.

Declaration of competing interest

The authors declare that they have no known competing financial interests or personal relationships that could have appeared to influence the work reported in this paper.

Acknowledgments

This work was financially supported by the Postgraduate Research & Practice Innovation Program of Jiangsu Province (No. KYCX21_2795), the Basic Science (Natural Science) Research Project of Colleges and Universities of Jiangsu Province (No. 21KJB540001), and Changzhou Sci&Tech Program (Nos. CJ20220180, CJ20210042), China.

References

[1] M. Luo, Z. Zhao, Y. Zhang, Nature 574 (2019) 81–85.
[2] Y. Chen, Z. Lai, X. Zhang, et al., Nat. Rev. Chem. 4 (2020) 243–256.
[3] G.F. Han, F. Li, A.I. Rykov, et al., Nat. Nanotechnol. 17 (2022) 403–407.
[4] S. Lan, B. Jing, C. Yu, et al., Small 18 (2022) 2105279.
[5] Y. Guo, T. Park, J.W. Yi, et al., Adv. Mater. 31 (2019) 1807134.
[6] Z. Xu, Z. Ao, M. Yang, et al., J. Hazard. Mater. 424 (2022) 127427.
[7] W.J. Jiang, T. Tang, Y. Zhang, et al., Acc. Chem. Res. 53 (2020) 1111–1123.
[8] X. Chu, K. Wang, W. Qian, et al., Coord. Chem. Rev. 477 (2023) 214952.
[9] Y. Chen, Z. Fan, Z. Luo, et al., Adv. Mater. 29 (2017) 1701331.
[10] L. Tian, Y. Liu, C. He, et al., Chem. Rec. 23 (2022) 202200213.
[11] L. Tian, H. Chen, X. Lu, et al., J. Colloid Interface Sci. 628 (2022) 663–672.
[12] H. Xu, J. Yuan, G. He, et al., Coord. Chem. Rev. 475 (2023) 214869.
[13] Q. Yun, Q. Lu, C. Li, et al., ACS Nano 13 (2019) 14329–14336.
[14] H. Xu, J. Li, X. Chu, Chem. Rec. 23 (2022) 202200244.
[15] J. Tosques, B. Honrado Guerreiro, M.H. Martin, et al., J. Alloy. Compd. 698 (2017) 725–730.
[16] T. Kwon, H. Hwang, Y.J. Sa, et al., Adv. Funct. Mater. 27 (2017) 1604688.
[17] H. Cheng, N. Yang, X. Liu, et al., Natl. Sci. Rev. 6 (2019) 955–961.
[18] X. Guo, H. Shang, J. Guo, et al., Appl. Surf. Sci. 481 (2019) 1532–1537.
[19] H. Xu, B. Huang, Y. Zhao, et al., Inorg. Chem. 61 (2022) 4533–4540.
[20] H. Xu, C. Wang, G. He, et al., Inorg. Chem. 61 (2022) 14224–14232.
[21] H. Xu, J. Li, X. Chu, et al., Nanoscale Horiz. 8 (2023) 441–452.
[22] X. Chu, L. Wang, H. Xu, Chem. Rec. 23 (2023) 202300013.
[23] H. Xu, Y. Zhao, Q. Wang, et al., Coord. Chem. Rev. 451 (2022) 214261.
[24] H. Xu, Y. Zhao, G. He, et al., Int. J. Hydrogen Energy 47 (2022) 14257–14279.
[25] Y. Zhao, H. Xing, Q. Wang, et al., Inorg. Chem. Front. 9 (2022) 2637–2643.
[26] B. Qiao, A. Wang, X. Yang, et al., Nat. Chem. 3 (2011) 634–641.
[27] H. Wei, X. Liu, A. Wang, et al., Nat. Commun. 5 (2014) 5634.
[28] L. Tian, Z. Huang, X. Lu, et al., Inorg. Chem. 62 (2023) 1659–1666.
[29] W.H. Lai, L.F. Zhang, W.B. Hua, et al., Angew. Chem. Int. Ed. 58 (2019) 11868–11873.
[30] Z. Jakub, J. Hulva, M. Meier, et al., Angew. Chem. Int. Ed. 58 (2019) 13961–13968.
[31] Y. Pan, Y. Chen, K. Wu, et al., Nat. Commun. 10 (2019) 4290.
[32] L. Tian, Z. Chen, T. Wang, et al., Nanoscale 15 (2023) 259–265.
[33] X. Xiao, Y. Gao, L. Zhang, et al., Adv. Mater. 32 (2020) e2003082.
[34] K. Wu, F. Zhan, R. Tu, et al., Chem. Commun. 56 (2020) 8916–8919 (Camb).
[35] H. Zhou, Y. Zhao, J. Gan, et al., J. Am. Chem. Soc. 142 (2020) 12643–12650.
[36] Y. Ma, Y. Ren, Y. Zhou, et al., Angew. Chem. Int. Ed. 59 (2020) 21613–21619.
[37] M. Tong, F. Sun, Y. Xie, et al., Angew. Chem. Int. Ed. 60 (2021) 14005–14012.
[38] L. Cui, L. Cui, Z. Li, et al., J. Mater. Chem. A 7 (2019) 16690–16695.

[39] Y. Zhao, X. Liu, D. Chen, et al., Sci. China Mater. 64 (2021) 1900–1909.
[40] Z. Yang, B. Chen, W. Chen, et al., Nat. Commun. 10 (2019) 3734.
[41] Y. Shang, X. Xu, B. Gao, et al., Chem. Soc. Rev. 50 (2021) 5281–5322.
[42] Y. Shang, X. Duan, S. Wang, et al., Chin. Chem. Lett. 33 (2022) 663–673.
[43] Y. Wang, S. Wang, S.L. Zhang, et al., Angew. Chem. Int. Ed. 59 (2020) 11918–11922.
[44] R. Zhou, X. Fan, X. Ke, et al., Nano Lett. 21 (2021) 4092–4098.
[45] C.J. Peng, G. Zeng, D.D. Ma, et al., ACS Appl. Mater. Interfaces 13 (2021) 20589–20597.
[46] J. Wang, C. Cheng, B. Huang, et al., Nano Lett. 21 (2021) 980–987.
[47] C. Dong, L. Cui, Y. Kong, et al., J. Phys. Chem. C 126 (2021) 102–109.
[48] L. An, Y. Hu, J. Li, et al., Adv. Mater. 34 (2022) e2202874.
[49] Z. Zhao, G. Lu, J. Phys. Chem. C 123 (2019) 4380–4387.
[50] D. Karapinar, N.T. Huan, N.Ranjbar Sahraie, et al., Angew. Chem. Int. Ed. 58 (2019) 15098–15103.
[51] A. Guan, Z. Chen, Y. Quan, et al., ACS Energy Lett. 5 (2020) 1044–1053.
[52] S. Chen, B. Wang, J. Zhu, et al., Nano Lett. 21 (2021) 7325–7331.
[53] J. Jiao, R. Lin, S. Liu, et al., Nat. Chem. 11 (2019) 222–228.
[54] Y. Cai, J. Fu, Y. Zhou, et al., Nat. Commun. 12 (2021) 586.
[55] T. Zheng, C. Liu, C. Guo, et al., Nat. Nanotechnol. 16 (2021) 1386–1393.
[56] H. Yang, Y. Wu, G. Li, et al., J. Am. Chem. Soc. 141 (2019) 12717–12723.
[57] M. Liu, S. Yin, T. Ren, et al., ACS Appl. Mater. Interfaces 13 (2021) 47458–47464.
[58] W. Zang, T. Yang, H. Zou, et al., ACS Catal. 9 (2019) 10166–10173.
[59] M. Arif, G. Yasin, L. Luo, et al., Appl. Catal. B: Environ. 265 (2020) 118559.
[60] N. Zhang, F. Zheng, B. Huang, et al., Adv. Mater. 32 (2020) 1906477.
[61] H. Xu, C. Wang, B. Huang, et al., Inorg. Chem. Front. 10 (2023) 2067–2074.
[62] P.Y. Liu, K. Shi, W.Z. Chen, et al., Appl. Catal. B: Environ. 287 (2021) 119956.
[63] Y. Xu, X. Liu, N. Cao, et al., Sustain. Mater. Technol. 27 (2021) e00229.
[64] C. Li, R. Xu, S. Ma, et al., Chem. Eng. J. 415 (2021) 129018.
[65] H. Lu, Y. Jiang, G. Xiao, et al., J. Colloid Interface Sci. 616 (2022) 539–547.
[66] L. Zhao, Y. Xiong, X. Wang, et al., Small 18 (2022) 2106939.
[67] C. Liu, Q. Li, C. Wu, et al., J. Am. Chem. Soc. 141 (2019) 2884–2888.
[68] J. Zhang, J. Lian, Q. Jiang, et al., Chem. Eng. J. 439 (2022) 135634.
[69] W. Deeloed, T. Priamushko, J. Cizek, et al., ACS Appl. Mater. Interfaces 14 (2022) 23307–23321.
[70] L. Tian, Z. Huang, W. Na, et al., Nanoscale 14 (2022) 15340–15347.
[71] Y. Zhu, J. Peng, X. Zhu, et al., Nano Lett. 21 (2021) 6625–6632.
[72] L. Tian, X. Pang, H. Xu, et al., Inorg. Chem. 61 (2022) 16944–16951.
[73] C. Wang, D. Liu, K. Zhang, et al., ACS Appl. Mater. Interfaces 14 (2022) 38669–38676.
[74] X. Chu, J. Li, H. Xu, et al., Dalt. Trans. 52 (2023) 245–259.
[75] T. He, W. Wang, X. Yang, et al., ACS Nano 15 (2021) 7348–7356.
[76] H. Ma, Z. Zheng, H. Zhao, et al., J. Mater. Chem. A 9 (2021) 23444–23450.
[77] L. Huang, S. Zaman, X. Tian, et al., Acc. Chem. Res. 54 (2021) 311–322.
[78] J. Li, Z. Zhou, H. Xu, et al., J. Colloid Interface Sci. 611 (2022) 523–532.
[79] L.Y. Zhang, C.X. Guo, H. Cao, et al., Chem. Eng. J. 431 (2022) 133237.
[80] X. Chu, J. Li, W. Qian, Chem. Rec. 23 (2023) 202200222.
[81] X. Zhao, X. Yu, S. Xin, et al., Appl. Catal. B: Environ. 301 (2022) 120785.
[82] L. Yang, X. Zhang, L. Yu, et al., Adv. Mater. 34 (2022) 2105410.
[83] H.S. Kim, C.H. Lee, J.H. Jang, et al., J. Mater. Chem. A 9 (2021) 4297–4309.
[84] N. Jia, Q. Xu, F. Zhao, et al., ACS Appl. Energy Mater. 1 (2018) 4982–4990.
[85] M. Qiao, Y. Wang, Q. Wang, et al., Angew. Chem. Int. Ed. 59 (2020) 2688–2694.
[86] Z. Jiang, W. Sun, H. Shang, et al., Energy Environ. Sci. 12 (2019) 3508–3514.
[87] J. Yang, W. Liu, M. Xu, et al., J. Am. Chem. Soc. 143 (2021) 14530–14539.
[88] H. Shang, X. Zhou, J. Dong, et al., Nat. Commun. 11 (2020) 3049.
[89] G. Han, Y. Zheng, X. Zhang, et al., Nano Energy 66 (2019) 104088.
[90] X. Wang, M. Zhu, G. Zeng, et al., Nanoscale 12 (2020) 9385–9391.
[91] D.P. Butcher, A.A. Gewirth, Nano Energy 29 (2016) 457–465.
[92] W.J. Sun, H.Q. Ji, L.X. Li, et al., Angew. Chem. Int. Ed. 60 (2021) 22933–22939.
[93] L. Liu, T. Xiao, H. Fu, et al., Appl. Catal. B: Environ. 323 (2023) 122181.
[94] H. Chen, C. Zhang, L. Sheng, et al., J Hazard. Mater. 434 (2022) 128892.
[95] J. Cai, Y. Wei, A. Cao, et al., Appl. Catal. B: Environ. 316 (2022) 121683.
[96] T. Zhu, Q. Chen, P. Liao, et al., Small 16 (2020) e2004526.
[97] H.X. Zhang, Q.L. Hong, J. Li, et al., Angew. Chem. Int. Ed. 58 (2019) 11752–11756.
[98] Y. Li, B. Li, D. Zhang, et al., ACS Nano 14 (2020) 10552–10561.
[99] G. Wang, C.T. He, R. Huang, et al., J. Am. Chem. Soc. 142 (2020) 19339–19345.
[100] Y. Liu, Y. Zhou, X. Zhou, et al., Chem. Eng. J. 407 (2021) 127180.
[101] J. He, L. Hu, C. Shao, et al., ACS Nano 15 (2021) 18006–18013.
[102] G. Sun, B. Xiao, H. Zheng, et al., J. Mater. Chem. A 9 (2021) 9735–9744.
[103] G. Zhang, D. Chen, N. Li, et al., Angew. Chem. Int. Ed. 59 (2020) 8255–8261.
[104] J. Wang, T. Heil, B. Zhu, et al., ACS Nano 14 (2020) 8584–8593.
[105] B.H. Lee, S. Park, M. Kim, et al., Nat. Mater. 18 (2019) 620–626.
[106] G. Wang, T. Zhang, W. Yu, et al., ACS Catal. 10 (2020) 5715–5722.
[107] Y. Zhang, M. Zhou, J. Hazard. Mater. 362 (2019) 436–450.
[108] Y. Pan, R. Qin, M. Hou, et al., Sep. Pur. Technol. 300 (2022) 121831.
[109] Z. Tang, Y. Liu, M. He, et al., Angew. Chem. Int. Ed. 58 (2019) 946–956.
[110] J.X. Fan, M.Y. Peng, H. Wang, et al., Adv. Mater. 31 (2019) e1808278.
[111] Y. Xiong, H. Li, C. Liu, et al., Adv. Mater. 34 (2022) e2110653.
[112] F. Chen, X.L. Wu, C. Shi, et al., Adv. Funct. Mater. 31 (2021) 2007877.
[113] J. Pan, B. Gao, P. Duan, et al., J. Mater. Chem. A 9 (2021) 11604–11613.
[114] M. Yang, Z. Hou, X. Zhang, et al., Environ. Sci. Tech. 56 (2022) 11635–11645.
[115] M. Yang, R. Wu, S. Cao, et al., Chem. Eng. J. 451 (2023) 138606.
[116] J. Zhang, C. Zheng, M. Zhang, et al., Nano Res. 13 (2020) 3082–3087.
[117] Z. Hou, L. Dai, Y. Liu, et al., Appl. Catal. B: Environ. 285 (2021) 119844.
[118] X. Hao, L. Dai, J. Deng, et al., J. Phys. Chem. C 125 (2021) 17696–17708.
[119] Y. Liu, J. Dai, N. Liu, et al., ACS Sustain. Chem. Eng. 9 (2021) 7255–7266.
[120] Q. Shen, P. Li, W. Chen, et al., Sci. China Mater. 65 (2021) 163–169.
[121] P. Basyach, A.K. Guha, S. Borthakur, et al., J. Mater. Chem. A 8 (2020) 12774–12789.
[122] T. Zhang, Z. Sun, S. Li, et al., Nat. Commun. 13 (2022) 6996.
[123] T. Zhang, X. Nie, W. Yu, et al., iScience 22 (2019) 97–108.
[124] T. Zhang, D. Zhang, X. Han, et al., J. Am. Chem. Soc. 140 (2018) 16936–16940.